Materials Research. 2023; 26:e20230008
DOI: https://doi.org/10.1590/1980-5373-MR-2023-0008

Implication of Pre-Aged Three Step T6 Treatment on the Properties of Granite and Silicon Nitride Particulates Reinforced Al7075 Matrix Composite

***B.S Sowrabh*[a], *B.M Gurumurthy*[a], *Y.M Shivaprakash*[a]*, *Sathya Shankara Sharma*[a]**

[a]*Department of Mechanical and Industrial Engineering, Manipal Institute of Technology, Manipal Academy of Higher Education, Manipal, Karnataka, India.*

Received: January 05, 2023; Revised: March 13, 2023; Accepted: March 30, 2023

In the current research Al7075 (Al-5.4Zn-2.6Mg) alloy and composite prepared by dispersing 2 wt.% granite powder and 3 wt.% Si_3N_4 in Al7075 are subjected to peak aging treatment at 100, 120 and 150^{0}C to obtain the maximum induced hardness by solid solution strengthening. In succession, by the results of peak aging treatment the alloy and composite are pre aged and heat treated by three step aging conditions. The results indicated that pre aged three step aging has resulted in enhanced alloy hardness of 185.6 VHN as compared to peak hardness of 142.9 at 100^{0}C resulting in 29.88% improvement. Moreover, the composite subjected to pre-aged three step aging has resulted in improved hardness to 197.6 VHN as compared to peak hardness of 153.5 at 100^{0}C resulting in 28.72% improvement. Also, the alloy and composite in this condition showed an improvement of 21.38% and 16.34% respectively in the UTS. Also, particularly composite displayed excellent wear characteristics as compared to as cast alloy. An interesting fact noticed in this work is that in three step aging the last step having higher temperature and longer duration of aging has resulted always a better hardness and hence has improved mechanical properties. This may be due to increased aging kinetics during heat treatment. The novel approach developed in this study will reduce the longer duration of conventional aging heat treatment and the energy consumption.

Keywords: *Al7075 alloy, step aging, pre aging, granite particle, silicon nitride, wear.*

1. Introduction

Aluminium alloys are widely preferred material for aerospace components because of their light weight, higher strength, good process ability, anti corrosive properties, and higher conductivity. Like steels these materials are can also be subjected to heat treatment to relieve stresses, improve the mechanical properties and ease the machining. Among different types of aluminium alloys 2000, 6000 and 7000 series alloys respond positively when subjected to heat treatment. The improvement in mechanical properties is achieved because of formation of small hard precipitates during commonly employed precipitation hardening or age hardening heat treatment process. The precipitates formed during this process cause the grains to lock into position and in turn enhances the hardness/strength of alloy.

7000 series aluminium alloys are widely used in aircraft structures due to the high strength and low density[1]. The high strength of the 7000 series alloys is due to the fine and uniformly distributed precipitates in the matrix which precipitate during the artificial aging. The usual precipitation sequence of the 7000 series Al alloys can be summarized as: solid solution-Guinier Preston zone-metastable η'- stable η ($MgZn_2$)[2]. For the peak aged (T6) 7000 series aluminium alloys, the η' phase is the main precipitate; however, for the over aged condition (T7) the η phase is the main precipitate[3,4].

In the recent past, aluminium matrix materials have emerged to satisfy the requirements of the applications in present industries as their properties can be easily tailor made to suit a specific demand of the application. Because of diverse properties, aluminium based composite materials hold potential for application in automotive, aerospace, sporting goods, defence, electronic, thermal management and in general engineering industries[5-7].

Because of numerous advantages of particulate reinforcements, they have been tried with the Al7075. M. Singh et al.[8,9] have reinforced granite powder particulates of size 50-150 µm and 10 wt.% in LM6 aluminium alloy for studying the high stress wear behaviour and dry sliding wear behaviour of composites. Satyanarayana et al.[10] have used granite and graphite particles of size 53 µm each to produce composites based on A356 aluminium alloy. The weight of graphite reinforced was 2 wt.% and that of granite was 4 wt.% in the alloy. They studied the wear parameters on friction performance of composites. Haq and Anand[11] have fabricated Al7075-Si_3N_4 composites by dispersing silicon nitride in varying quantity in the range 2-8 wt.% in steps of 2. The objective of their study was to understand the microhardness of composites. Mistry and Gohil[12] have used Si_3N_4 of size 10-40 µm to produce Al7075 matrix composites. The quantity of reinforcement introduced varied from 4-12 wt.% in steps of 4. The investigation focus was to understand the wear and friction behaviour of composites under heat treated conditions.

*e-mail: prakash.ym@manipal.edu

Ramesh and Keshavamurthy[13,14] and Ramesh et al.[15] have Ni-P coated Si_3N_4 (2-20 μm) and reinforced them with varying quantity in the range 4-10 wt.% in steps of 2 in Al6061 alloy. They studied slurry erosive wear behaviour, dry sliding wear and Influence of forging on mechanical properties of Al6061-Si_3N_4 composites. Kumar et al.[16,17] produced Al2618 alloy matrix based Si_3N_4, aluminium nitride (AlN) and ZrB_2 reinforced composites for understanding the mechanical behaviour, corrosion resistance and applied ANOVA for understanding variable that will significantly affect the wear of these composites. The combined quantity of reinforcements introduced in these composites was in the range 2-8 wt.%.

The three stages in precipitation hardening are- solutionizing, quenching and aging. During solutionizing the temperature is raised between 430-540^{0}C above solvus temperature and held for certain duration to dissolve all the elements of alloy into a solid solution. The quenching involves cooling at a faster rate to produce a super saturated solid solution and aging will enable the appearance of coherent precipitates that aid for strengthening the alloy by interfering with dislocation movement.

Heat treatment is a process carried out on the materials to increase the grain growth and tensile strength related properties[18]. The dendritic structure, impurities, and intermetallic particles in wrought and as-cast alloys remarkably give rise to negative influence on mechanical response and limit several end-use applications. Therefore, heat treatment as an indispensable step in multiple processing sectors is developed in today's industry to eliminate the above defects as much as possible. Among those heat treatment methods, aging treatment is the most common and effective approach that can not only reduce or eliminate the micro-stress in matrix after quenching process but improve the strength and hardness of alloy by modifying the fraction number, size, and distribution of intermetallic particles[19]. The heat treatment has a clear influence on the alloy's topographical responds to the ambient conditions[20]. The multiple-step aging process is a heat treatment process derived from solution-aging treatment[21]. Longer duration in isothermal heat treatment (single step aging) of alloys for industrial purpose can be eliminated by adapting the multiple step aging treatment for achieving similar mechanical properties[22-24]. Generally, the first step aging is a low temperature process, in which fine distribution of Guinier Preston zones takes place. In the subsequent higher temperature steps, complete precipitation of strengthening phase will be achieved[25,26]. Good processing method combined with an appropriate aging condition can significantly promote the optimization of microstructure and performance of the alloys[27-29].

2. Materials and Casting

2.1. Materials

2.1.1. Al7075

Aluminium alloy 7075 has a good blend of strength, ductility, toughness, higher strength to weight ratio, very good electrical and thermal conductance, good fatigue strength and corrosion resistance. It is one of the 7xxx series alloy which has wide applications in aerospace, aircraft, electronic and automobile parts[29-32].

The density of as received Al7075 is 2.83 g/cc, and its chemical composition has been given in Table 1.

2.1.2. Granite powder (GP)

Granite belongs to the igneous rock family. The density of the granite powder used is 2.6 g/cc and compressive strength is around 210 MPa. Granite powder was obtained from the polishing units and the chemical properties were found by wet method as per IS2720:1983. The details of different chemical elements found have been shown in Table 2. Average particle size of the granite particulates is found to be as 40 μm as confirmed by the particle size analysis. Figure 1 shows the photograph of granite slab and the derived granite powder from it.

Table 1. Chemical composition of Al7075.

Element	Zn	Mg	Cu	Si	Fe	Mn	Cr	Ti	Al
wt. %	5.4	2.6	1.5	0.4	0.5	0.3	0.22	0.2	Bal.

Table 2. Chemical composition of granite powder.

Element	SiO_2	Al_2O_3	Fe_2O_3	CaO	MgO	Na_2O	K_2O	TiO_2
wt. %	73.18	14.23	1.64	0.92	5.01	3.09	1.59	0.23

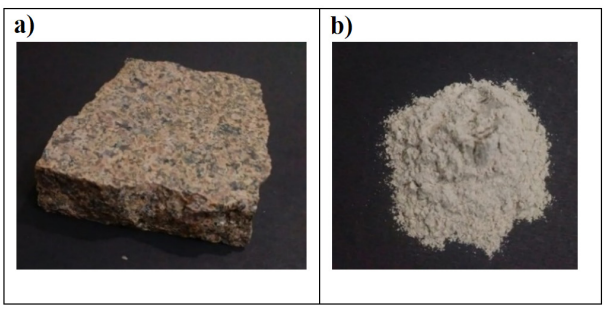

Figure 1. (a) granite slab (b) granite powder reinforcement.

To clean granite powder, it is taken in a beaker and demineralized water is added to it to get a liquid slurry. This liquid slurry is stirred for 10 minutes. After stirring, water with granite powder is filtered using filter paper. The pH value of the filtered water is noted down. This process is repeated till the pH value of water reaches 7. Increase in pH value of water is the indication of removal of contaminants and other minerals from the granite powder. The process equipment adapted is as shown in Figure 2.

2.1.3. Silicon Nitride

The Si_3N_4 reinforcement used had properties as depicted in Table 3. This reinforcement has a density of 3.44 g/cc and particle size in the range 20-30 µm with irregular shaped particulates.

2.2. Casting of composite

The mold surfaces are polished by emery paper and cleaned by acetone to remove dust, grease, and any other foreign particles. The surfaces are applied with the paste formed by mixture of graphite, acetone, and water for ease of removal of casting avoiding sticking of molten material to die walls. The dies are then preheated to 550^0C for 2 h. in a muffle furnace to aid for uniform cooling of the melt as it is poured into it. The graphite crucible loaded with ingots (as received at T6 condition) of Al7075 alloy is taken into melting furnace and the temperature of furnace is raised to 800^0C. Into the melt at this temperature alkaline powder (10 g) is added to remove the slag and then further added with hexa chloro ethane (C_2Cl_6, 10 g) to degasify the melt to break the pores in it. The alloy melt is now poured at 800^0C into the preheated molds to cast the cylindrical and rectangular specimens.

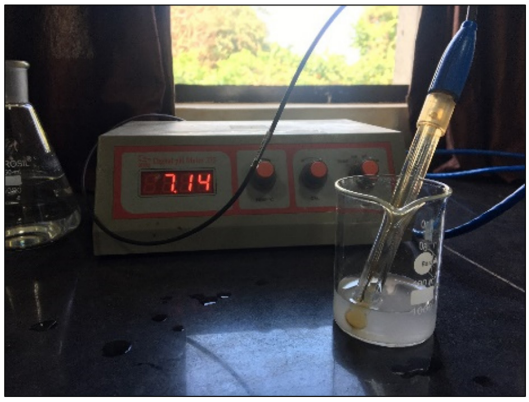

Figure 2. Process of cleaning granite powder.

To cast the composite, after degasifying and slag removal the melt at 800^0C is stirred at 150 rpm by using a stainless-steel stirrer blade coated with graphite to create a deep vortex. The pre heated granite powder (2 wt.%), Si_3N_4 (3 wt.%) reinforcements are now added to the melt vortex through a stainless-steel feeder and stirred for 10 min. The melt is now brought to semisolid state by cooling it to 600^0C and stirred for 10 minutes at 250 rpm and then again melt temperature is increased to 800^0C and continued to stir again for 10 minutes at 150 rpm. The composite melt is now poured at 800^0C into the preheated molds to cast the cylindrical and rectangular composite specimens. The castings of composite are as shown in Figure 3.

As can be observed in Figure 4 the reinforcements are uniformly distributed in the matrix. Figure 5 depicts the SEM-EDAX of the composite confirming the presence of major chemical components.

2.3. Experimental approach

2.3.1. Mechanical characterization of as cast alloy and composite

2.3.1.1. Hardness test

The Vickers hardness test is carried out on cast alloy and composite as per ASTM E92-17 standard. In this test a diamond indenter is used, and 100 g(f) load is applied for 15 sec. The 320, 400, 600, 1000, 1500 and 2000 grit emery paper was used to polish the test specimen to decrease the machining scratches and the effects of surface defects if any on the sample, followed by fine polishing using a velvet cloth on surface with disc speed of 545 rpm. A diamond suspension of 3 and 1 µm size is used in sequence on cloth while fine polishing. The test was carried out at ambient weather (30^0C) and the hardness was measured at five spots on the surface of each sample to calculate the average VHN. The results of the hardness test is tabulated in Table 4.

Table 3. Major chemical components of silicon nitride powder.

Element	Al	Fe	Ca	Mn	Pb
ppm	380	260	200	1.2	0.48

Table 4. Average hardness values (VHN) of cast alloy and composite.

Material	VHN
Al7075 (A)	90
Composite (C)	115

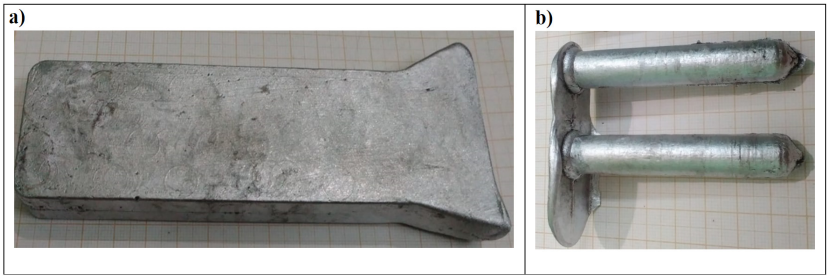

Figure 3. Composite castings.

2.3.1.2. Tensile test

The tensile test on alloy and composite specimens is carried out as per ASTM-E8M standard. The test speed adapted is 2 mm/min. The results of tensile test carried out on as cast composite specimen in four trials indicated an average UTS of 204.9 MPa. The results of the tensile test are tabulated in Table 5.

2.3.2. Heat treatment

The different heat treatment conditions employed in this study have been listed in Table 6. The Table also shows the abbreviation used for each of these treatments. Table 7 shows the designation used for alloy and composite samples subjected to age hardening under different aging parameters.

2.3.2.1. Peak aging treatment of as cast alloy and composite

The as cast alloy and composite is subjected to solutionizing and aging heat treatment in sequence as per the heat treatment curves shown in Figure 6, to determine the time required to attain peak hardness and corresponding peak hardness (VHN). The as cast alloy and composite samples are aged at 100, 120 and 150^{0}C respectively. The induced peak hardness for each aging temperature at different time duration for as cast alloy and composite during aging have been tabulated in Table 8.

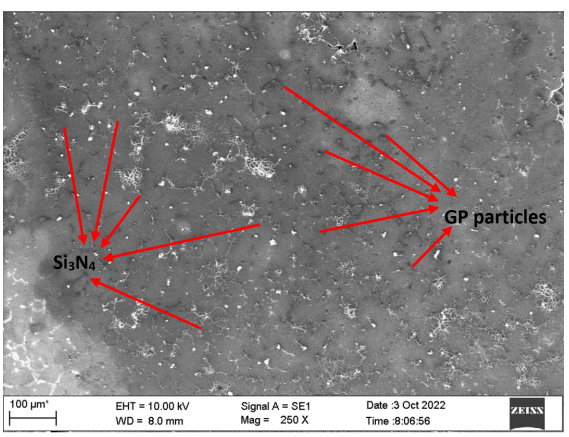

Figure 4. Morphology of distribution of reinforcements in the matrix.

2.3.2.2. Step aging

In step aging, the time for aging is calculated depending on the number of steps. In three steps aging the time of aging at each step is taken as one third of that of single step aging at that temperature so that overall duration remains same as that of single step aging.

Table 5. Average UTS of as cast alloy and composite.

Material	UTS (MPa)
Al7075 (A)	181.0
Composite (C)	204.9

Table 6. Heat treatment conditions and their abbreviations.

Heat treatment condition	Abbreviation
Solution Treatment	ST
Aging Treatment	AT
Pre Aging Treatment	PAT
First Step Aging Treatment	FSAT
Second Step Aging Treatment	SSAT
Third Step Aging Treatment	TSAT

Table 7. Alloy/composite sample designation for different age hardening parameters.

Sample ID		Heat treatment parameter
Alloy	Composite	
A1	C1	ST-470^{0}C, 2h; AT-100^{0}C
A2	C2	ST-470^{0}C, 2h; AT-120^{0}C
A3	C3	ST-470^{0}C, 2h; AT-150^{0}C

Table 8. Peak hardness and time to attain peak hardness in samples.

Sample	Time to attain peak hardness (h)	Peak hardness (VHN)
A1	t_{A1} = 6.5	142.9
A2	t_{A2} =4.5	139.4
A3	t_{A2} =3.0	137.9
C1	t_{C1} = 5.5	153.5
C2	t_{C2} =3.5	149.6
C3	t_{C3} =2.5	145.8

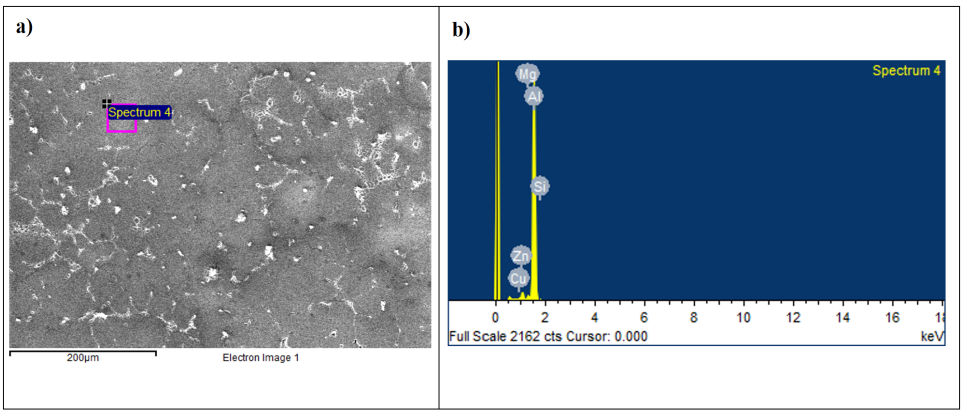

Figure 5. SEM-EDAX of the composite.

In normal conditions time duration of each step is calculated directly as mentioned above so that longer duration is taken at lower temperature, whereas shorter duration at higher temperature. In interchanged condition, time is interchanged (swapped) so that at lower temperature higher temperature peak aging duration is considered and vice versa. The alloy and composite samples subjected to different step aging parameters have been designated as shown in Table 9.

2.3.2.3. Combined pre age hardening and three step aging heat treatment

The alloy and composite are subjected to pre aging treatment followed by three step aging treatment as per the heat treatment curves shown in Figures 7-10. The pre aging is carried out at 500^{0}C for 8 h and then furnace cooled. In the first trial temperature and duration of aging of first step, second step and third step are fixed as shown in Figures 7 and 9, whereas in the second trial the durations of FS and TS are swapped as shown in Figures 8 and 10. The durations are chosen based on the results of peak aging treatment. The split up and total duration along with attained hardness for three step aging has been summarized in Tables 10-11.

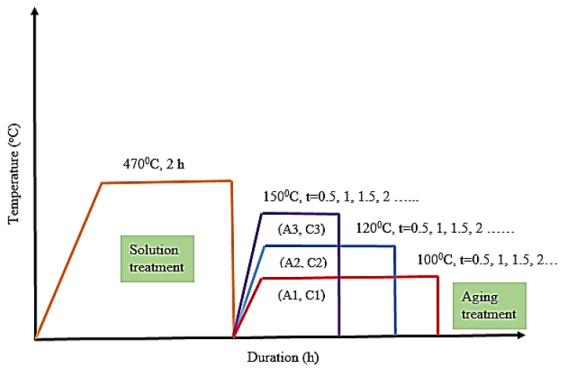

Figure 6. Heat treatment curves for finding peak hardness of samples.

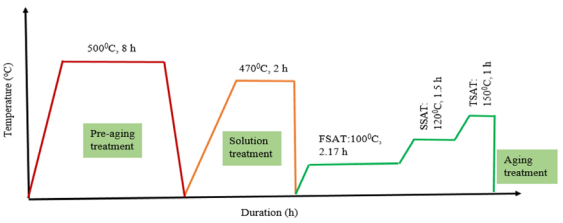

Figure 7. Heat treatment curve for finding hardness of samples A4.

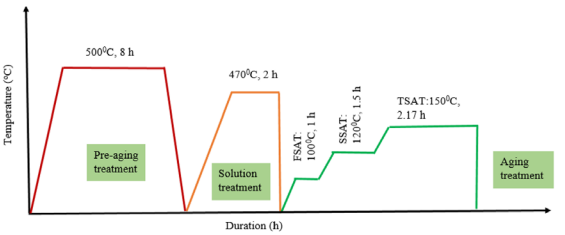

Figure 8. Heat treatment curve for finding hardness of samples A5.

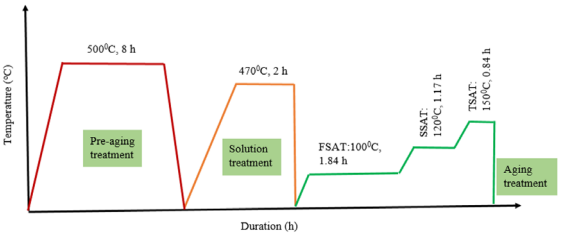

Figure 9. Heat treatment curve for finding hardness of samples C4.

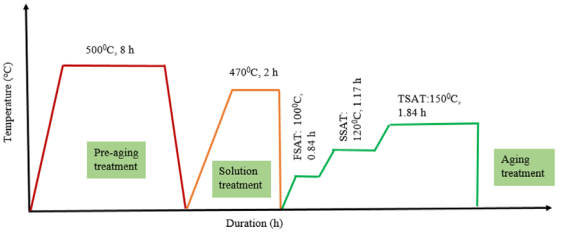

Figure 10. Heat treatment curve for finding hardness of samples C5.

Table 9. Alloy/composite sample designation for different step aging parameters.

Sample ID	Step aging parameter
A4	PAT-500^{0}C, 8 h; ST-470^{0}C, 2 h; FSAT-100^{0}C,2.17 h; SSAT-120^{0}C, 1.5 h; TSAT-150^{0}C,1 h
A5	PAT-500^{0}C, 8 h; ST-470^{0}C, 2h; FSAT-100^{0}C,1 h; SSAT-120^{0}C, 1.5 h; TSAT-150^{0}C, 2.17 h
C4	PAT-500^{0}C, 8 h; ST-470^{0}C, 2h; FSAT-100^{0}C,1.84 h; SSAT-120^{0}C, 1.17 h; TSAT-150^{0}C,0.84 h
C5	PAT-500^{0}C, 8 h; ST-470^{0}C, 2h; FSAT-100^{0}C,0.84 h; SSAT-120^{0}C, 1.17 h; TSAT-150^{0}C, 1.84 h

Table 10. Hardness of as cast alloy subjected to pre aging and three step aging heat treatment.

Sample	Duration of FS (h)	Duration of SS (h)	Duration of TS (h)	Total duration of aging process (h)	Hardness (VHN)
A4	2.17	1.5	1	4.67	180.3
A5	1	1.5	2.17	4.67	185.6

Table 11. Hardness of as cast composite subjected to pre aging and three step aging heat treatment.

Sample	Duration of FS (h)	Duration of SS (h)	Duration of TS (h)	Total duration of aging process (h)	Hardness (VHN)
C4	1.84	1.17	0.84	3.85	188.5
C5	0.84	1.17	1.84	3.85	197.6

2.3.2.4. Comparison of hardness of samples

Table 12 shows the hardness values achieved for all the samples during heat treatment variations given. 3 steps aging interchanged condition shows excellent result for alloy (185.6 VHN) and composite (197.6 VHN) respectively.

3. Mechanical characterization of A5 and C5 samples

3.1. Tension test

The tension test is carried out on A5 and C5 specimen (having maximum peak hardness among all) very similar to mentioned in section 2.3.1.2 and the average of four trials on the specimen showed an UTS of 219.75 and 238.4 MPa for A5 and C5 specimens respectively.

3.2. Wear test

The wear tests were conducted on A5 and C5 samples as per ASTM G-99 standards in air under the laboratory condition having a relative humidity of 80 to 85% and temperature ranging between 25 to 29^{0}C.The duration of single test was 30 min. The test specimen contact surface and disc surface were polished with silicon carbide emery paper of 600 grit for smooth contact between them prior to the conduction of each test. The specimens were cleaned with ethanol solution before and after each test. After each 5 minutes during the test the specimen mass was measured to know the mass loss by using a high precision electronic weighing machine (Infra digital balance, Model: IN2011) having a resolution of 0.001mg. Also, the track of disc and specimen surface was regularly cleaned by soft cotton cloth to avoid the entrapment of wear debris.

The test specimen is a cylindrical pin (8 mm diameter and 27 mm length) that was held with its axis perpendicular to the surface of the disc, and one end of pin slid against the disc in a dry friction condition, under a constant axial load applied with a dead weight. For testing specimens in both as cast and in heat treated conditions, a sliding velocity of 0.4188 m/sec (200 rpm) and 0.5235 m/sec (250 rpm) is selected. The applied normal load was 20, 30, 40 and 50 N.

The parameters of wear like wear rate (W_r), volumetric wear rate (W_v) and specific wear rate (W_s) were determined based on the mass loss Δm, of the specimen that is measured at the end of each 5 minutes during the test having one specific condition of load, speed, and track diameter. The results of wear test carried out on pre-aged and triple step aged alloy(A5) and composite (C5) are shown in Tables 13-28.

Table 12. Hardness of all test samples.

Condition	Sample ID	VHN
ST-470^{0}C, 2h; AT-100^{0}C	A1	142.9
ST-470^{0}C, 2h; AT-120^{0}C	A2	139.4
ST-470^{0}C, 2h; AT-150^{0}C	A3	137.9
ST-470^{0}C, 2h; AT-100^{0}C	C1	153.5
ST-470^{0}C, 2h; AT-120^{0}C	C2	149.6
ST-470^{0}C, 2h; AT-150^{0}C	C3	145.8
PAT-500^{0}C, 8 h; ST-470^{0}C, 2 h; FSAT-100^{0}C, 2.17 h; SSAT-120^{0}C, 1.5 h; TSAT-150^{0}C, 1 h	A4	180.3
PAT-500^{0}C, 8 h; ST-470^{0}C, 2 h; FSAT-100^{0}C,1h; SSAT-120^{0}C, 1.5 h; TSAT-150^{0}C, 2.17 h	A5	185.6
PAT-500^{0}C, 8 h; ST-470^{0}C, 2 h; FSAT-100^{0}C, 2.17 h; SSAT-120^{0}C, 1.5 h; TSAT-150^{0}C, 1 h	C4	188.5
PAT-500^{0}C, 8 h; ST-470^{0}C, 2 h; FSAT-100^{0}C,1h; SSAT-120^{0}C, 1.5 h; TSAT-150^{0}C, 2.17 h	C5	197.6

Table 13. Results of wear test on pre aged and triple step aged alloy (A5) under the normal load of 20 N and 200 rpm disc speed.

Triple step aged Al7075						
Load=20 N, 200 rpm, ρ = 2.83 g/cc						
Vs=0.4188 m/sec						
Δm x 10^{-3} (g)	t (sec)	μ	SD x 10^3 (m)	W_r x 10^{-7} (N/m)	W_v x 10^{-12} (m^3/sec)	W_s x 10^{-13} (m^3/N-m)
1	300	0.432	0.126	0.796	1.178	1.4062
2	600	0.474	0.251	0.796	1.178	1.4062
4	900	0.459	0.377	1.061	1.570	1.8750
5	1200	0.475	0.503	0.995	1.472	1.7578
7	1500	0.432	0.628	1.114	1.649	1.9687
8	1800	0.441	0.754	1.061	1.570	1.8750

Table 14. Results of wear test on pre aged and triple step aged alloy (A5) under the normal load of 20 N and 250 rpm disc speed.

Triple step aged Al7075						
Load=20 N, 250 rpm, ρ = 2.83 g/cc						
Vs=0.5235 m/sec						
$\Delta m \times 10^{-3}$ (g)	t (sec)	μ	SD x 10^{3} (m)	$W_r \times 10^{-7}$ (N/m)	$W_v \times 10^{-12}$ (m^3/sec)	$W_s \times 10^{-13}$ (m^3/N-m)
2	300	0.434	0.157	1.273	2.356	2.2500
3	600	0.476	0.314	0.955	1.767	1.6875
5	900	0.461	0.471	1.061	1.963	1.8750
6	1200	0.476	0.628	0.955	1.767	1.6875
8	1500	0.434	0.785	1.019	1.885	1.8000
10	1800	0.442	0.942	1.061	1.963	1.8750

Table 15. Results of wear test on pre aged and triple step aged alloy (A5) under the normal load of 30 N and 200 rpm disc speed.

Triple step aged Al7075						
Load=30 N, 200 rpm, ρ = 2.83 g/cc						
Vs=0.4188 m/sec						
$\Delta m \times 10^{-3}$ (g)	t (sec)	μ	SD x 10^{3} (m)	$W_r \times 10^{-7}$ (N/m)	$W_v \times 10^{-12}$ (m^3/sec)	$W_s \times 10^{-13}$ (m^3/N-m)
2	300	0.576	0.126	1.592	2.356	1.875
3	600	0.477	0.251	1.194	1.767	1.406
5	900	0.543	0.377	1.327	1.963	1.562
7	1200	0.588	0.503	1.393	2.061	1.641
8	1500	0.512	0.628	1.273	1.885	1.500
10	1800	0.597	0.754	1.327	1.963	1.562

Table 16. Results of wear test on pre aged and triple step aged alloy (A5) under the normal load of 30 N and 250 rpm disc speed.

Triple step aged Al7075						
Load=30 N, 250 rpm, ρ = 2.83 g/cc						
Vs=0.5235 m/sec						
$\Delta m \times 10^{-3}$ (g)	t (sec)	μ	SD x 10^{3} (m)	$W_r \times 10^{-7}$ (N/m)	$W_v \times 10^{-12}$ (m^3/sec)	$W_s \times 10^{-13}$ (m^3/N-m)
3	300	0.578	0.157	1.910	3.534	2.250
4	600	0.479	0.314	1.273	2.356	1.500
6	900	0.545	0.471	1.273	2.356	1.500
8	1200	0.589	0.628	1.273	2.356	1.500
10	1500	0.514	0.785	1.273	2.356	1.500
12	1800	0.598	0.942	1.273	2.356	1.500

Table 17. Results of wear test on pre aged and triple step aged alloy (A5) under the normal load of 40 N and 200 rpm disc speed.

Triple step aged Al7075						
Load=40 N, 200 rpm, ρ = 2.83 g/cc						
Vs=0.4188 m/sec						
$\Delta m \times 10^{-3}$ (g)	t (sec)	μ	SD x 10^{3} (m)	$W_r \times 10^{-7}$ (N/m)	$W_v \times 10^{-12}$ (m^3/sec)	$W_s \times 10^{-13}$ (m^3/N-m)
3	300	0.598	0.126	2.388	3.534	2.109
4	600	0.581	0.251	1.592	2.356	1.406
6	900	0.634	0.377	1.592	2.356	1.406
8	1200	0.583	0.503	1.592	2.356	1.406
10	1500	0.561	0.628	1.592	2.356	1.406
12	1800	0.554	0.754	1.592	2.356	1.406

Table 18. Results of wear test on pre aged and triple step aged alloy (A5) under the normal load of 40 N and 250 rpm disc speed.

Triple step aged Al7075						
Load=40 N, 250 rpm, ρ = 2.83 g/cc						
Vs=0.5235 m/sec						
$\Delta m \times 10^{-3}$ (g)	t (sec)	μ	SD x 10^{3} (m)	$W_r \times 10^{-7}$ (N/m)	$W_v \times 10^{-12}$ (m^3/sec)	$W_s \times 10^{-13}$ (m^3/N-m)
4	300	0.6	0.157	2.547	4.711	2.250
5	600	0.598	0.314	1.592	2.945	1.406
7	900	0.636	0.471	1.486	2.748	1.312
9	1200	0.585	0.628	1.433	2.650	1.266
11	1500	0.564	0.785	1.401	2.591	1.237
14	1800	0.556	0.942	1.486	2.748	1.312

Table 19. Results of wear test on pre aged and triple step aged alloy (A5) under the normal load of 50 N and 200 rpm disc speed.

Triple step aged Al7075						
Load=50 N, 200 rpm, ρ = 2.83 g/cc						
Vs=0.4188 m/sec						
$\Delta m \times 10^{-3}$ (g)	t (sec)	μ	SD x 10^{3} (m)	$W_r \times 10^{-7}$ (N/m)	$W_v \times 10^{-12}$ (m^3/sec)	$W_s \times 10^{-13}$ (m^3/N-m)
4	300	0.598	0.126	3.184	4.711	2.2500
6	600	0.623	0.251	2.388	3.534	1.6875
8	900	0.634	0.377	2.122	3.141	1.5000
10	1200	0.563	0.503	1.990	2.945	1.4062
13	1500	0.567	0.628	2.069	3.062	1.4625
14	1800	0.622	0.754	1.857	2.748	1.3125

Table 20. Results of wear test on pre aged and triple step aged alloy (A5) under the normal load of 50 N and 250 rpm disc speed.

Triple step aged Al7075						
Load=50 N, 250 rpm, ρ = 2.83 g/cc						
Vs=0.5235 m/sec						
$\Delta m \times 10^{-3}$ (g)	t (sec)	μ	SD x 10^{3} (m)	$W_r \times 10^{-7}$ (N/m)	$W_v \times 10^{-12}$ (m^3/sec)	$W_s \times 10^{-13}$ (m^3/N-m)
5	300	0.611	0.157	3.184	5.889	2.2500
7	600	0.625	0.314	2.229	4.122	1.5750
9	900	0.636	0.471	1.910	3.534	1.3500
11	1200	0.565	0.628	1.751	3.239	1.2375
14	1500	0.569	0.785	1.783	3.298	1.2600
15	1800	0.625	0.942	1.592	2.945	1.1250

Table 21. Results of wear test on pre aged and triple step aged composite (C5) under the normal load of 20 N and 200 rpm disc speed.

Triple step aged Al7075 composite						
Load=20 N, 200 rpm, ρ = 3.1 g/cc						
Vs=0.4188 m/sec						
$\Delta m \times 10^{-3}$ (g)	t (sec)	μ	SD x 10^{3} (m)	$W_r \times 10^{-7}$ (N/m)	$W_v \times 10^{-12}$ (m^3/sec)	$W_s \times 10^{-13}$ (m^3/N-m)
1	300	0.435	0.126	0.796	1.178	1.4062
1	600	0.468	0.251	0.398	0.589	0.7031
3	900	0.473	0.377	0.796	1.178	1.4062
4	1200	0.482	0.503	0.796	1.178	1.4062
5	1500	0.485	0.628	0.796	1.178	1.4062
6	1800	0.487	0.754	0.796	1.178	1.4062

Table 22. Results of wear test on pre aged and triple step aged composite (C5) under the normal load of 20 N and 250 rpm disc speed.

Triple step aged Al7075 composite						
Load=20 N, 250 rpm, ρ = 3.1 g/cc						
Vs=0.5235 m/sec						
$\Delta m \times 10^{-3}$ (g)	t (sec)	μ	SD x 10^{3} (m)	$W_r \times 10^{-7}$ (N/m)	$W_v \times 10^{-12}$ (m^3/sec)	$W_s \times 10^{-13}$ (m^3/N-m)
2	300	0.471	0.157	1.273	2.356	2.2500
3	600	0.472	0.314	0.955	1.767	1.6875
4	900	0.473	0.471	0.849	1.570	1.5000
6	1200	0.475	0.628	0.955	1.767	1.6875
7	1500	0.476	0.785	0.891	1.649	1.5750
8	1800	0.481	0.942	0.849	1.570	1.5000

Table 23. Results of wear test on pre aged and triple step aged composite (C5) under the normal load of 30 N and 200 rpm disc speed.

Triple step aged Al7075 composite						
Load=30 N, 200 rpm, ρ =3.1 g/cc						
Vs=0.4188 m/sec						
$\Delta m \times 10^{-3}$ (g)	t (sec)	μ	SD x 10^{3} (m)	$W_r \times 10^{-7}$ (N/m)	$W_v \times 10^{-12}$ (m^3/sec)	$W_s \times 10^{-13}$ (m^3/N-m)
2	300	0.553	0.126	1.592	2.356	1.875
3	600	0.551	0.251	1.194	1.767	1.406
4	900	0.554	0.377	1.061	1.570	1.250
4	1200	0.556	0.503	0.796	1.178	0.937
5	1500	0.553	0.628	0.796	1.178	0.937
7	1800	0.555	0.754	0.929	1.374	1.094

Table 24. Results of wear test on pre aged and triple step aged composite (C5) under the normal load of 30 N and 250 rpm disc speed.

Triple step aged Al7075 composite						
Load=30 N, 250 rpm, ρ = 3.1g/cc						
Vs=0.5235 m/sec						
$\Delta m \times 10^{-3}$ (g)	t (sec)	μ	SD x 10^{3} (m)	$W_r \times 10^{-7}$ (N/m)	$W_v \times 10^{-12}$ (m^3/sec)	$W_s \times 10^{-13}$ (m^3/N-m)
2	300	0.575	0.157	1.273	2.356	1.500
4	600	0.577	0.314	1.273	2.356	1.500
5	900	0.578	0.471	1.061	1.963	1.250
6	1200	0.581	0.628	0.955	1.767	1.125
8	1500	0.582	0.785	1.019	1.885	1.200
10	1800	0.584	0.942	1.061	1.963	1.250

Table 25. Results of wear test on pre aged and triple step aged composite (C5) under the normal load of 40 N and 200 rpm disc speed.

Triple step aged Al7075 composite						
Load=40 N, 200 rpm, ρ =3.1 g/cc						
Vs=0.4188 m/sec						
$\Delta m \times 10^{-3}$ (g)	t (sec)	μ	SD x 10^{3} (m)	$W_r \times 10^{-7}$ (N/m)	$W_v \times 10^{-12}$ (m^3/sec)	$W_s \times 10^{-13}$ (m^3/N-m)
1	300	0.588	0.126	0.796	1.178	0.703
3	600	0.589	0.251	1.194	1.767	1.055
4	900	0.591	0.377	1.061	1.570	0.937
5	1200	0.593	0.503	0.995	1.472	0.879
7	1500	0.587	0.628	1.114	1.649	0.984
9	1800	0.590	0.754	1.194	1.767	1.055

Table 26. Results of wear test on pre aged and triple step aged composite (C5) under the normal load of 40 N and 250 rpm disc speed.

Triple step aged Al7075 composite						
Load=40 N, 250 rpm, ρ =3.1 g/cc						
Vs=0.5235 m/sec						
$\Delta m \times 10^{-3}$ (g)	t (sec)	μ	SD x 10^{3} (m)	$W_r \times 10^{-7}$ (N/m)	$W_v \times 10^{-12}$ (m^3/sec)	$W_s \times 10^{-13}$ (m^3/N-m)
3	300	0.592	0.157	1.910	3.534	1.687
5	600	0.593	0.314	1.592	2.945	1.406
8	900	0.595	0.471	1.698	3.141	1.500
9	1200	0.597	0.628	1.433	2.650	1.266
10	1500	0.599	0.785	1.273	2.356	1.125
11	1800	0.612	0.942	1.167	2.159	1.031

Table 27. Results of wear test on pre aged and triple step aged composite (C5) under the normal load of 50 N and 200 rpm disc speed.

Triple step aged Al7075 composite						
Load=50 N, 200 rpm, ρ = 3.1 g/cc						
Vs=0.4188 m/sec						
$\Delta m \times 10^{-3}$ (g)	t (sec)	μ	SD x 10^{3} (m)	$W_r \times 10^{-7}$ (N/m)	$W_v \times 10^{-12}$ (m^3/sec)	$W_s \times 10^{-13}$ (m^3/N-m)
3	300	0.604	0.126	2.388	3.534	1.6875
5	600	0.605	0.251	1.990	2.945	1.4062
6	900	0.607	0.377	1.592	2.356	1.1250
8	1200	0.608	0.503	1.592	2.356	1.1250
10	1500	0.609	0.628	1.592	2.356	1.1250
11	1800	0.609	0.754	1.459	2.159	1.0312

Table 28. Results of wear test on pre aged and triple step aged composite (C5) under the normal load of 50 N and 250 rpm disc speed.

Triple step aged Al7075 composite						
Load=50 N, 250 rpm, ρ =3.1 g/cc						
Vs=0.5235 m/sec						
$\Delta m \times 10^{-3}$ (g)	t (sec)	μ	SD x 10^{3} (m)	$W_r \times 10^{-7}$ (N/m)	$W_v \times 10^{-12}$ (m^3/sec)	$W_s \times 10^{-13}$ (m^3/N-m)
6	300	0.612	0.157	3.820	7.067	2.7000
8	600	0.616	0.314	2.547	4.711	1.8000
9	900	0.618	0.471	1.910	3.534	1.3500
11	1200	0.619	0.628	1.751	3.239	1.2375
12	1500	0.621	0.785	1.528	2.827	1.0800
13	1800	0.624	0.942	1.380	2.552	0.9750

4. Results and Discussion

4.1. Step aging

Step aging is an alternative aging procedure used to artificially age non-ferrous metals to increase their tensile strength and hardness in comparison to single-step aging. Depending on the aging dynamics of the alloy system under consideration, the aging process in step aging may consist of two to three steps. While aging at a higher temperature (T3) provides modest property enhancement at a shorter aging duration, aging at a very low temperature (T1) requires a very lengthy aging duration with outstanding property enhancement. For step aging, a range of temperatures is chosen rather than aging at one temperature. When using a single-step aging process, "t" refers to the number of hours needed to reach peak hardness at the specified aging temperature. Therefore, at lower aging temperatures, 't' is longer, whereas at higher aging temperatures, 't' is shorter. Step aging, which consists of three processes, is used to try and improve the property. Time for aging in three stages is regarded as t/3, accordingly. Surprisingly, if the time duration is switched, positive outcomes rather than typical durations are shown. For instance, three aging temperatures of 100, 120, and 150^0C are taken into consideration while aging Al7075 alloy (A5) or composite (C5). In the beginning,

aging temperature is provided with single-step aging. After the initial pre-aging, 3 stage aging are provided in various combinations of time (normal and interchanged timings).

4.2. Hardness

Figure 11 compares the variance in hardness of specimens under peak, two-step, and three-step aging with and without pre-aging. In contrast to greater aging temperatures, lesser aging temperatures have produced the highest hardness (S1), as can be shown (S2 and S3). This is explained by a rise in intermediate zones during precipitation, a rise in finer intermetallic, and a decline in interparticle distances[33-35]. After peak aging circumstances, the hardness value declines because of excessive aging, which causes precipitates to coarsen. The alloy generally becomes softer as it ages. The increased rate of solid atom diffusion throughout the matrix results in an increase in aging rate as temperature rises.

For industrial reasons, a longer peak age treatment period is not usually preferred. As a result, multi-stage heat treatments have been advocated as a quicker way to achieve equivalent mechanical properties[36-38]. These treatments rely on two steps, the first at a low temperature to finely distribute Guinier Preston zones and the second at a higher temperature to finish precipitation[38,39].

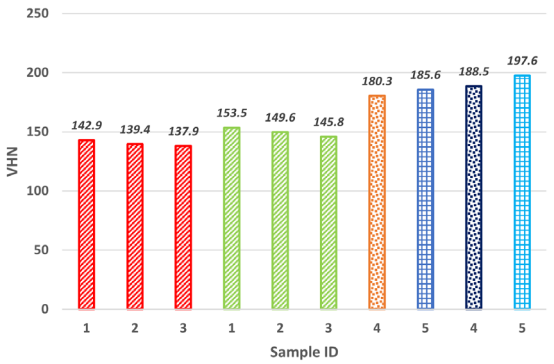

Figure 11. Peak hardness at 100, 120 and 150^{0}C for Al7075 and composite (1, 2, 3: single step aging), hardness in combined pre aging and three step aging for Al7075(A5) and composite(C5) (4-normal condition, 5-interchanged condition).

The alloy hardness has increased from pre-aging to three-stage aging, reaching 185.6 VHN. The composite hardness has increased from pre-aging to three-stage aging, reaching 197.6 VHN. Enhanced hardness is always the result of graded age treatments, with the last aging step having a greater temperature and longer duration.

The data above suggests that heat treatment has a significant impact on the hardness of matrix alloy.

4.3. Tensile strength

For triple step aged Al7075, the improvement in tensile strength is attributed to the presence of hard secondary phases on soft matrix leading to alloy strengthening. This also helps to decrease grain size of the matrix resulting further improvement of mechanical properties[40]. When load is applied, the presence of intermetallic contributes to dislocation pileup, increasing back stress, and work hardening the matrix due to restricted plastic flow in the ductile matrix. The synergistic effect of dislocation interaction with the intermetallic and grain boundary provides a positive contribution to alloy strengthening[41,42].

4.3.1. Fracture analysis

Figure 12 is the SEM micrograph of the peak aged, three-step interchanged alloy specimen depicting uniform and finer dendrites of the same size covered in river patterns that are evenly dispersed throughout the matrix. Finer dendrites of a consistent size demonstrate that the specimen is at its maximal age. The failure specimen is represented by a well-distributed smaller river pattern in the dendrites, which is strengthened by plastic deformation during fracture. There is no evidence to suggest that a brittle domination

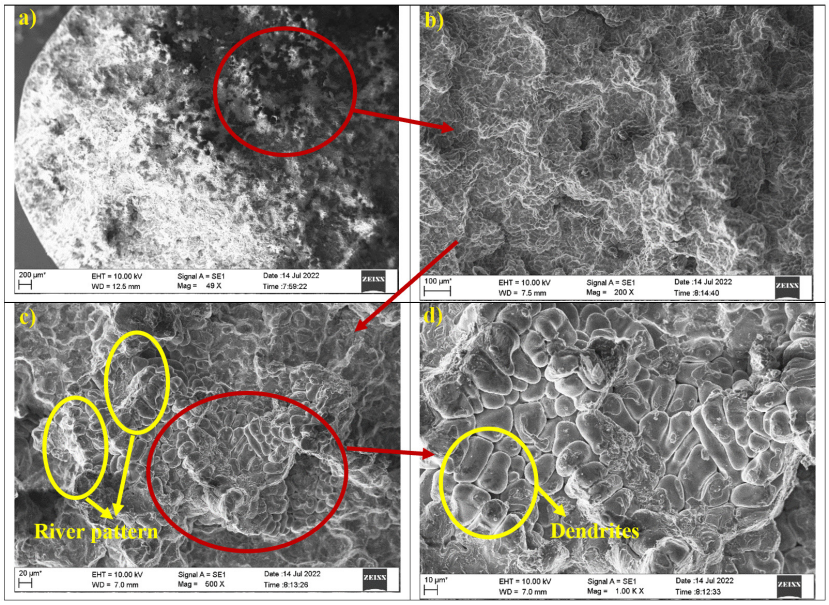

Figure 12. SEM micrographs of fracture surface of A5 tensile specimen after fracture.

failure has taken place. Additionally, there is no evidence of trans granular failure. According to the micrograph, ductile dominates nucleation. Figure 13 shows the SEM-EDAX of A5 specimen.

Figure 14 shows the SEM micrograph of the peak-aged, three-step interchanged composite specimen, which shows that the matrix having equally distributed fine dendrites of the same size that are encased in river patterns.

The particles from the second phase were dispersed along the grain boundaries. During the tensile test, these second phase particles prevented grain deformation. When the second phase particles separated from the grain boundary, they created tiny pores that continued to expand and eventually started a crack that led to fracture. As a result, the fracture happened in the direction of the load. There were no visible dimples on the fracture surface, which was made up of micro-porosities and dendritic structure.

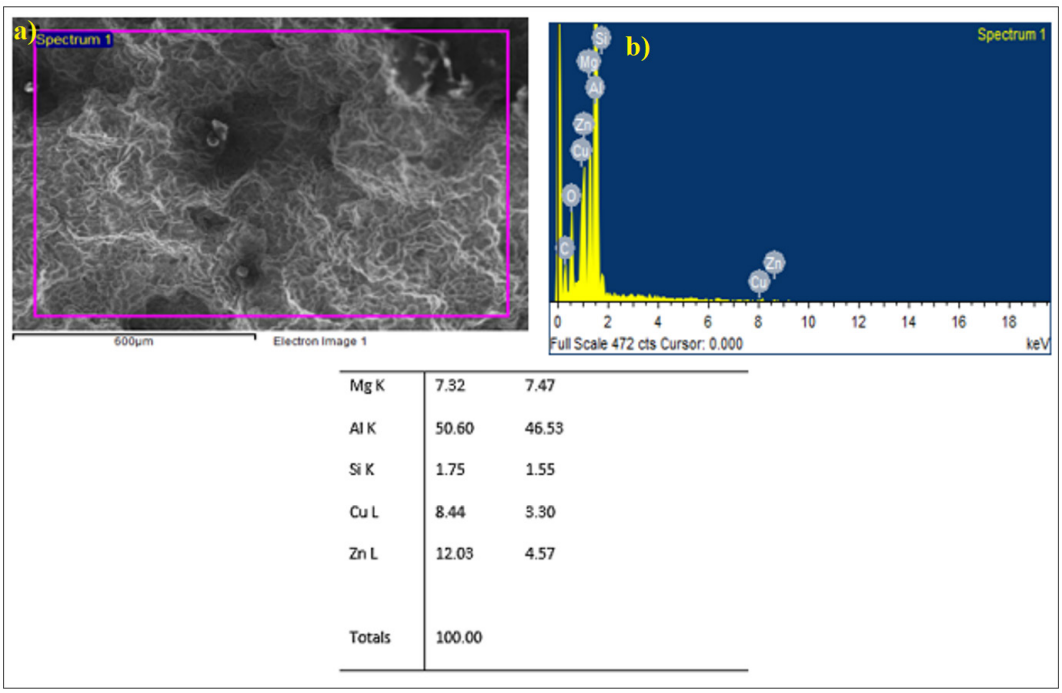

Mg K	7.32	7.47
Al K	50.60	46.53
Si K	1.75	1.55
Cu L	8.44	3.30
Zn L	12.03	4.57
Totals	100.00	

Figure 13. SEM-EDAX spectrum of A5 tensile specimen after fracture.

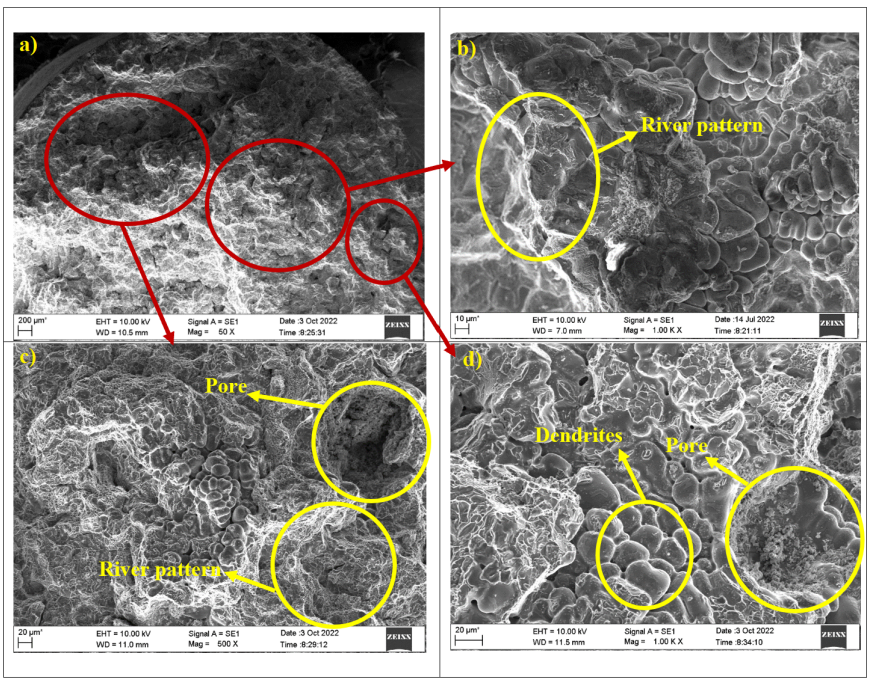

Figure 14. SEM micrographs of fracture surface of C5 tensile specimen after fracture.

Figure 15 demonstrates that the randomly selected spot comprises the constituents of the alloy Al 7075 as well as those produced because of reinforcements.

4.4. Wear behaviour

The variation of different wear parameters for pre aged and triple step aged alloy (A5) and composite (C5) has been shown in Figures 16-22. Mass loss and wear rate both increased as the sliding distance increased. As the typical load is raised with a corresponding rise in mass loss, it is found that the average wear rate has risen. Composite specimens are shown to have lower mass loss and wear rates than alloy specimens. As disc speed increased, the rate of wear increased as well (Figure 16). In comparison to composite materials, the average wear rate is lower and has grown with an increase in the size of normal load. Additionally, the average wear rate has noticeably risen at higher speeds (Figure 17). Figure 18 shows that the specific wear rate for composite materials reduces for larger loads and stays constant for higher sliding distances. Comparing composites to alloys, the specific wear rate is lower for composites. Additionally, as speed has increased, the average specific wear rate has gone up. As the sliding distance increased for both speeds, the volumetric wear rate decreased. Comparatively speaking, composite has a smaller magnitude. For the fastest speed, it is noticed that the average volumetric wear rate is larger (Figure 19). The average volumetric wear rate fluctuation with normal load is shown in Figure 20. Both larger load and faster speed have the propensity to raise the average volumetric wear rate. The average coefficient of friction has increased because of increasing load and speed values, as illustrated in Figure 21. The average coefficient of friction has increased significantly along with the sliding distance. For composites, as seen in Figure 22, its magnitude is greater.

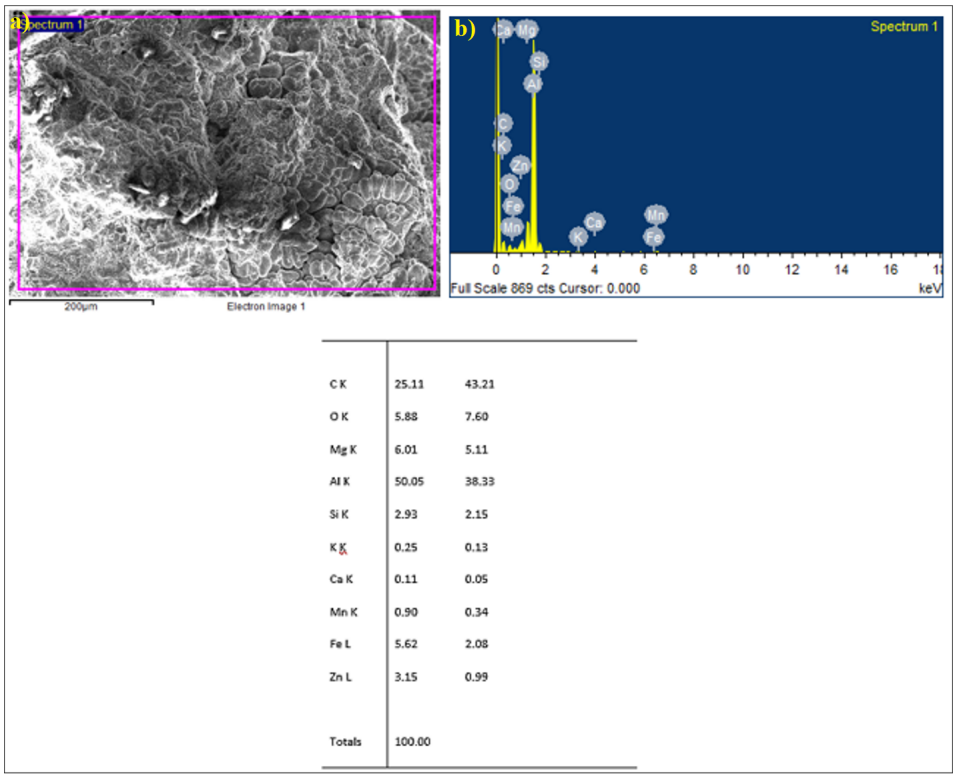

Figure 15. SEM-EDAX spectrum of C5 tensile specimen after fracture.

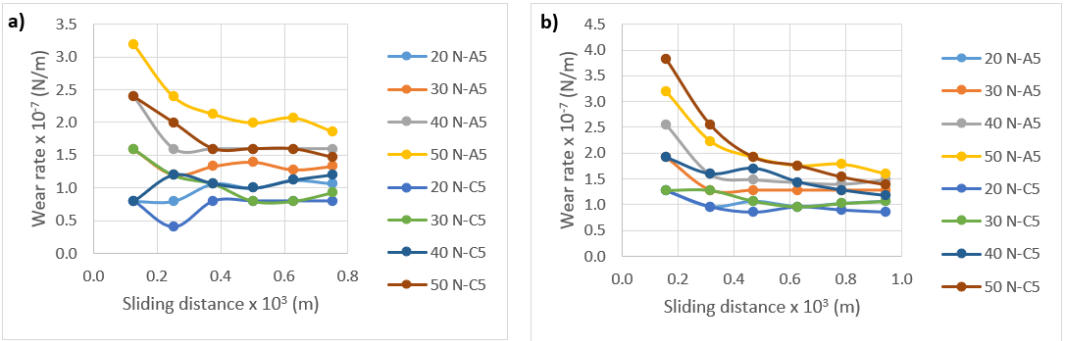

Figure 16. Variation of wear rate with sliding distance of A5 and C5 specimen at (a) 200 rpm and (b) 250 rpm.

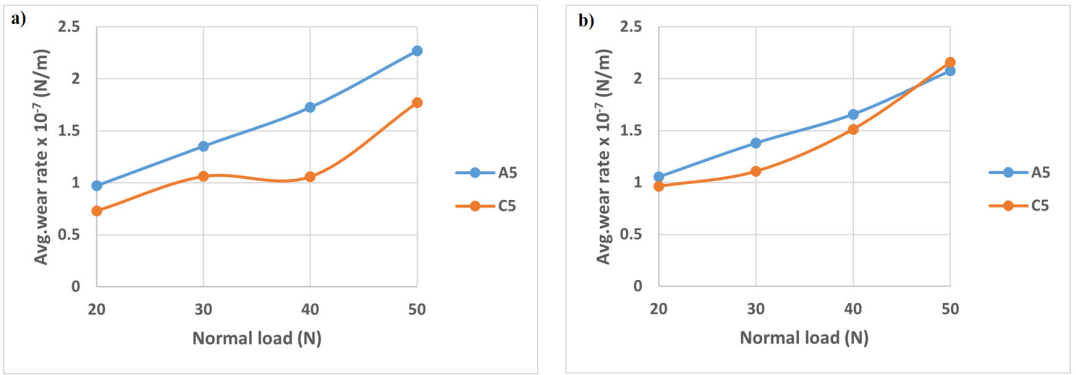

Figure 17. Variation of avg. wear rate with normal load of A5 and C5 specimen at (a) 200 rpm and (b) 250 rpm.

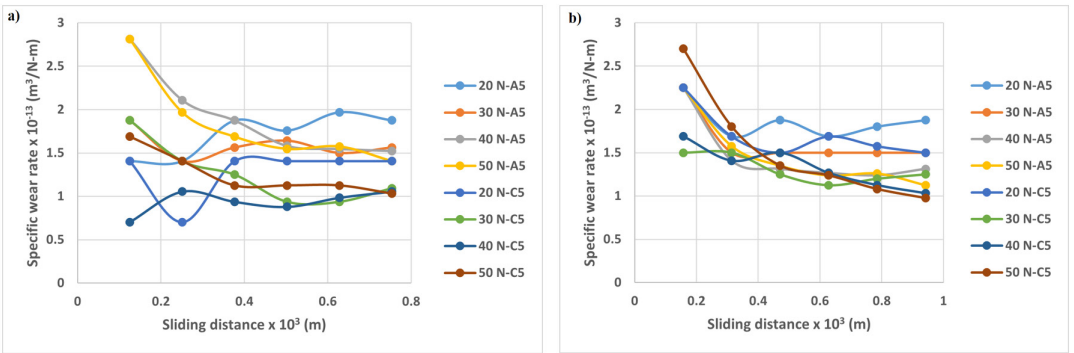

Figure 18. Variation of specific wear rate with sliding distance of A5 and C5 specimen at (a) 200 rpm and (b) 250 rpm.

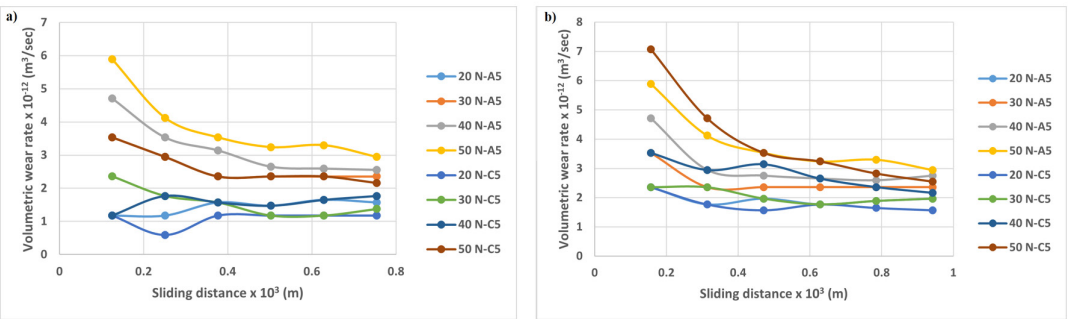

Figure 19. Variation of volumetric wear rate with sliding distance of A5 and C5 specimen at (a) 200 rpm and (b) 250 rpm.

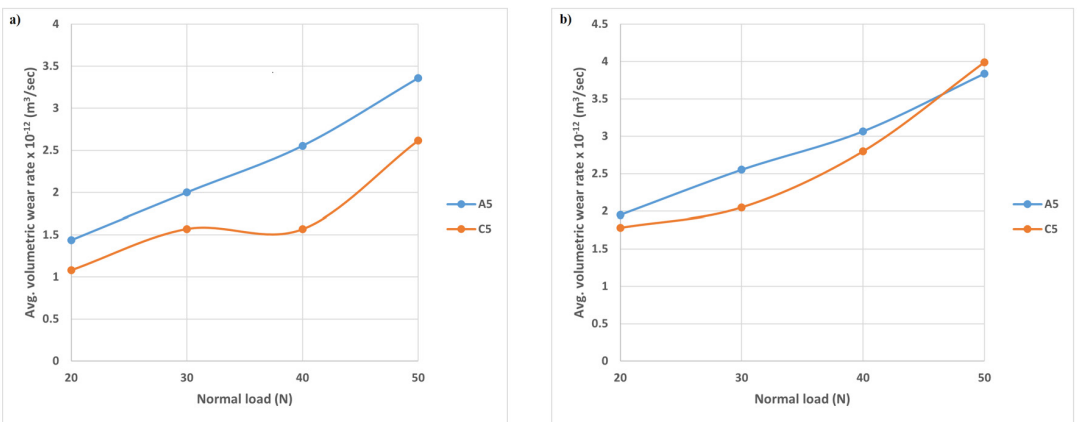

Figure 20. Variation of avg. volumetric wear rate with normal load of A5 and C5 specimen at (a) 200 rpm and (b) 250 rpm.

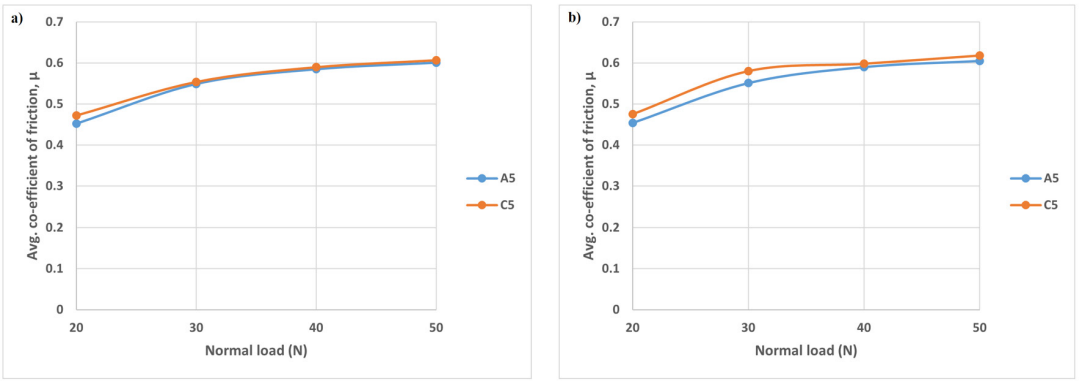

Figure 21. Variation of avg. co-efficient of friction with normal load of A5 and C5 specimen at (a) 200 rpm and (b) 250 rpm.

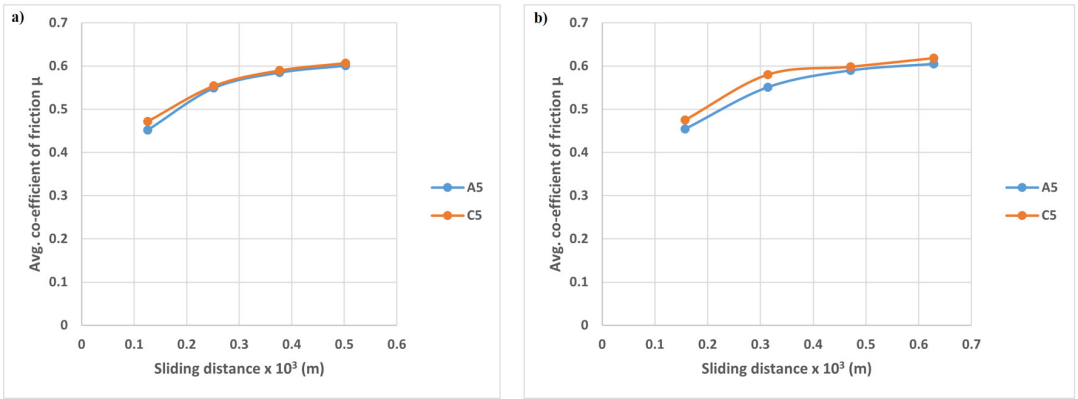

Figure 22. Variation of avg. co-efficient of friction with sliding distance of A5 and C5 specimen at (a) 200 rpm and (b) 250 rpm.

5. Conclusions

The Al7075 alloy and its composite underwent three steps of T6 aging treatment after being pre-aged. Peak hardness of the alloy increased by roughly 29.88% to 185.6 VHN from 142.9 VHN achieved by similar direct solution treatment followed by aging treatment. Accordingly, the increase in hardness for composite is from 153.5 VHN to 197.6 VHN, or a 28.72% improvement.

Due to a combination of pre-aging and a three-step T6 age process, the C5 specimen has 6.46% more hardness than the A5 specimen. As a result of the existence of hard secondary phases on a soft matrix during three-step aging, the alloy's tensile strength has increased, and this variation trend resembles the peak hardness distribution pattern. In addition, the presence of hard-reinforced granite powder and Si_3N_4 particles has helped the composite (C5) to carry more weight, leading to an 8.48% increase in strength compared to the A5 specimen. In comparison to the A5 equivalent, this composite has shown enhanced wear properties.

The presence of finer, more evenly spaced, smaller rivers indicates that plastic deformation predominates in the tensile failure mechanism. In terms of decreased aging time and energy, the innovative pre aging supported stepped aging treatment examined here outperforms standard aging treatment.

References

1. Hatch JE, editor. Aluminium properties and physical metallurgy. Materials Park: American Society for Metals; 1984.
2. Sha G, Cerezo A. Early-stage precipitation in Al–Zn–Mg–Cu alloy (7050). Acta Mater. 2004;52:4503.
3. Chinh NQ, Lendvai J, Ping DH, Hono K. The effect of Cu on mechanical and precipitation properties of AI-Zn-Mg alloys. J Alloys Compd. 2004;378:52.
4. Ou BL, Yang JG, Wei MY. Effect of homogenization and aging treatment on mechanical properties and stress-corrosion cracking of 7050 alloys. Metall Mater Trans A Phys Metall Mater Sci. 2007;38:1760.
5. Singh M, Prasad BK, Mondal DP, Jha AK. Dry sliding wear behaviour of an aluminium alloy–granite particle composite. Tribol Int. 2001;34:557-67.
6. Das S, Saraswathi YL, Mondal DP. Erosive-corrosive wear of aluminium alloy composites: influence of slurry composition and speed. Wear. 2006;261:180-90.
7. Wu GH, Dou ZY, Jiang LT, Cao JH. Damping properties of aluminium matrix–fly ash composites. Mater Lett. 2006;60(24):2945-8.
8. Singh M, Modi OP, Dasgupta R, Jha AK. High stress abrasive wear behaviour of aluminium alloy–granite particle composite. Wear. 1999;233:455-61.
9. Singh M, Prasad BK, Mondal DP, Jha AK. Dry sliding wear behaviour of an aluminium alloy–granite particle composite. Tribol Int. 2001;34(8):557-67.
10. Satyanarayana T, Rao PS, Krishna MG. Influence of wear parameters on friction performance of A356 aluminium–graphite/granite particles reinforced metal matrix hybrid composites. Heliyon. 2019;5(6):e01770.

11. Haq MI, Anand A. Microhardness studies on stir cast AA7075-Si_3N_4 based composites. Mater Today Proc. 2018;5(9):19916-22.
12. Mistry JM, Gohil PP. Experimental investigations on wear and friction behaviour of Si_3N_{4p} reinforced heat-treated aluminium matrix composites produced using electromagnetic stir casting process. Compos Part B Eng. 2019;161:190-204.
13. Ramesh CS, Keshavamurthy R. Slurry erosive wear behavior of Ni–P coated Si_3N_4 reinforced Al6061 composites. Mater Des. 2011;32:1833-43.
14. Ramesh CS, Keshavamurthy R. Influence of forging on mechanical properties of Ni–P coated Si_3N_4 reinforced Al6061 composites. Mater Sci Eng A. 2012;551:59-66.
15. Ramesh CS, Keshavamurthy R, Channabasappa BH, Pramod S. Friction and wear behavior of Ni–P coated Si_3N_4 reinforced Al6061 composites. Tribol Int. 2010;43:623-34.
16. Kumar NM, Kumaran SS, Kumaraswamidhas LA. An investigation of mechanical properties and corrosion resistance of Al2618 alloy reinforced with Si_3N_4, AlN and ZrB_2 composites. J Alloys Compd. 2015;652:244-9.
17. Kumar NM, Kumaran SS, Kumaraswamidhas LA. Aerospace application on Al 2618 with reinforced – Si_3N_4, AlN and Zrb_2 in-situ Composites. J Alloys Compd. 2016;672(5):238-50.
18. Alphonse M, Raja VKB, Vivek MS, Raj NVSD, Darshan MSS, Bharmal P. Effect of heat treatment on mechanical properties of forged aluminium alloy AA2219. Mater Today Proc. 2021;44:3811-5.
19. Zhang Z, Deng Y, Ye L, Zhu W, Wang F, Jiang K et al. Influence of aging treatments on the strength and localized corrosion resistance of aged Al-Zn-Mg-Cu alloy. J Alloys Compd. 2020;846:156223.
20. Fageehi YA, Saminathan R, Venugopal G, Valder J, Kumar H, Ravishankar KS. Effect of thermal and surface chemical treatment on the cyclic oxidation behaviour of 7039 aluminium alloy used in aerospace armor applications. Mater Today Proc. 2021;42(Pt 2):343-9.
21. Liu Z, Du Z, Jiang H, Gong T, Cui X, Liu J et al. Microstructure evolution and corresponding tensile properties of Ti–5Al–5Mo–5V–1Cr–1Fe alloy controlling by multi-heat treatments. Prog Nat Sci Mater Int. 2021;31(5):731-41.
22. Omer K, Abolhasani A, Kim S, Nikdejad T, Butcher C, Wells M et al. Process parameters for hot stamping of AA7075 and D-7xxx to achieve high performance aged products. J Mater Process Technol. 2018;257:170-9. https://doi.org/10.1016/j.jmatprotec.2018.02.039.
23. Osterreicher JA, Kirov G, Gerstl SS, Mukeli E, Grabner F, Kumar M. Stabilization of 7xxx aluminium alloys. J Alloys Compd. 2018;740:167-73. https://doi.org/10.1016/j.jallcom.2018.01.003.
24. Lee Y-S, Koh D-H, Kim H-W, Ahn Y-S. Improved bake hardening response of Al-Zn-Mg-Cu alloy through pre-aging treatment. Scr Mater. 2018;147:45-9. https://doi.org/10.1016/j.scriptamat.2017.12.030.
25. Stemper L, Tunes MA, Dumitraschkewitz P, Mendez-Martin F, Tosone R, Marchand D et al. Giant hardening response in AlMgZn(Cu) alloys. Acta Mater. 2021;206:116617. http://dx.doi.org/10.1016/j.actamat.2020.116617.
26. Jiang F, Huang J, Jiang Y, Xu C. Effects of quenching rate and over-aging on microstructures, mechanical properties and corrosion resistance of an Al-Zn-Mg (7046A) alloy. J Alloys Compd. 2021;854:157272.
27. Liu S, Zhang M, Li Q, Zhu Q, Song H, Wu X et al. Effect of quenching rate on strengthening behaviour of an Al-Zn-Mg-Cu alloy during natural aging. Mater Sci Eng A. 2020;793:139900.
28. Zhou L, Chen K, Chen S, Ding Y, Fan S. Correlation between stress corrosion cracking resistance and grain-boundary precipitates of a new generation high Zn-containing 7056 aluminium alloy by non-isothermal aging and re-aging heat treatment. J Alloys Compd. 2021;850:156717.
29. Sowrabh BS, Gurumurthy BM, Shivaprakash YM, Sharma SS. Reinforcements, production techniques and property analysis of AA7075 matrix composites-a critical review. Manuf Rev. 2021;8:31.
30. Shivaprakash YM, Ramu HC, Chiranjivee, Kumar R, Kumar D. Experimental studies on Al (5.7% Zn) alloy based hybrid MMC. IOP Conf Ser Mater Sci Eng. 2018;310:012004.
31. Akhlaghi F, Bidaki AZ. Influence of graphite content on the dry sliding and oil impregnated sliding wear behavior of Al 2024-graphite composites produced by in situ powder metallurgy method. Wear. 2009;266:37-45.
32. Prashant SN, Madeva N, Auradi V. Preparation and evaluation of mechanical and wear properties of 6061Al reinforced with graphite particulate metal matrix composite. Int J Metall Mater Sci Eng. 2012;2(3):85-95.
33. Wolverton C. Crystal structure and stability of complex precipitate phases in AleCueMge(Si) and AleZneMg alloys. Acta Mater. 2001;49(16):3129-42. https://doi.org/10.1016/S1359-6454(01)00229-4.
34. Li J, Peng Z, Li C, Jia Z, Chen W, Zheng Z. Mechanical properties, corrosion behaviours and microstructures of 7075 aluminium alloy with various aging treatments. Trans Nonferrous Met Soc China. 2008;18(4):755-62. https://doi.org/10.1016/S1003-6326(08)60130-2.
35. Österreicher JA, Tunes MA, Grabner F, Arnoldt A, Kremmer T, Pogatscher S et al. Warm-forming of pre-aged Al-Zn-Mg-Cu alloy sheet. Mater Des. 2020;193:108837. http://dx.doi.org/10.1016/j.matdes.2020.108837.
36. Omer K, Abolhasani A, Kim S, Nikdejad T, Butcher C, Wells M et al. Process parameters for hot stamping of AA7075 and D-7xxx to achieve high performance aged products. J Mater Process Technol. 2018;257:170-9. https://doi.org/10.1016/j.jmatprotec.2018.02.039.
37. Osterreicher JA, Kirov G, Gerstl SS, Mukeli E, Grabner F, Kumar M. Stabilization of 7xxx aluminium alloys. J Alloys Compd. 2018;740:167-73. http://dx.doi.org/10.1016/j.jallcom.2018.01.003.
38. Lee Y-S, Koh D-H, Kim H-W, Ahn Y-S. Improved bake hardening response of Al-Zn-Mg-Cu alloy through pre-aging treatment. Scr Mater. 2018;147:45-9. https://doi.org/10.1016/j.scriptamat.2017.12.030.
39. Stemper L, Tunes MA, Dumitraschkewitz P, Mendez-Martin F, Tosone R, Marchand D et al. Giant hardening response in AlMgZn(Cu) alloys. Acta Mater. 2021;206:116617.
40. Shivaprakash YM, Gurumurthy BM, Siddhartha MA, Kumar NMS, Dutta A. Studies on mild steel particulates reinforced duralumin composite fabricated through powder metallurgy route. Int J Mech Prod Eng Res Dev. 2019;9(2):903-20.
41. Ibrahim MF, Ammar HR, Samuel AM, Soliman MS, Almajid A, Samuel FH. Mechanical properties and fracture of Al–15 vol.% B_4C based metal matrix composites. Int J Cast Met Res. 2014;27(1):7-14.
42. Auradi V, Rajesh GL, Kori SA. Processing of B_4C particulate reinforced 6061aluminium matrix composites by melt stirring involving two-step addition. Procedia Mater Sci. 2014;6:1068-76.